HHS Public Access

Author manuscript

Nat Neurosci. Author manuscript; available in PMC 2013 March 01.

Published in final edited form as:

Nat Neurosci. 2012 September ; 15(9): 1227–1235. doi:10.1038/nn.3178.

Alzheimer Amyloid-β Oligomer Bound to Post-Synaptic Prion Protein Activates Fyn to Impair Neurons

Ji Won Um[1], **Haakon B. Nygaard**[1], **Jacqueline K. Heiss**[1], **Mikhail A. Kostylev**[1], **Massimiliano Stagi**[1], **Alexander Vortmeyer**[2], **Thomas Wisniewski**[3], **Erik C. Gunther**[1], and **Stephen M. Strittmatter**[1]

[1]Cellular Neuroscience, Neurodegeneration and Repair Program, Departments of Neurology and Neurobiology, Yale University School of Medicine, New Haven, CT 06536 USA.

[2]Department of Pathology, Yale University School of Medicine, New Haven, CT 06536 USA.

[3]Department of Neurology, New York University School of Medicine, 550 First Avenue, New York, NY 10016, USA.

SUMMARY

Amyloid-beta (Aβ) oligomers are thought to trigger Alzheimer's disease (AD) pathophysiology. Cellular Prion Protein (PrP^C) selectively binds oligomeric Aβ and can mediate AD-related phenotypes. Here, we examined the specificity, distribution and signaling from Aβ/PrP complexes, seeking to explain how they might alter the function of NMDA receptors in neurons. PrP^C is enriched in post-synaptic densities, and Aβ/PrP^C interaction leads to Fyn kinase activation. Soluble Aβ assemblies derived from human AD brain interact with PrP^C to activate Fyn. Aβ engagement of PrP^C/Fyn signaling yields phosphorylation of the NR2B subunit of NMDA-receptors, which is coupled to an initial increase and then loss of surface NMDA-receptors. Aβ-induced LDH release and dendritic spine loss require both PrP^C and Fyn, and human familial AD transgene-induced convulsive seizures do not occur in mice lacking PrP^C. These results delineate an Aβ oligomer signal transduction pathway requiring PrP^C and Fyn to alter synaptic function with relevance to AD.

INTRODUCTION

Genetic, pathological and biomarker studies of Alzheimer's Disease (AD) provide support for Amyloid-Beta (Aβ) as a key factor in pathogenesis. More specifically, oligomeric species of Aβ peptide (Aβo) are thought to trigger synaptic dysfunction, neurodegeneration and dementia[1–4]. Key is delineation of the pathway(s) leading from Aβo to downstream pathogenic events. We identified cellular Prion Protein (PrP^C) as an oligomer-specific, high-

Correspondence and requests for materials should be addressed to S.M.S., (stephen.strittmatter@yale.edu).

AUTHOR CONTRIBUTIONS: J.U., H.B.N., J.K.H., M.A.K., M.S., A.V., E.C.G. and S.M.S. designed various aspects of the research. J.U., H.B.N., J.K.H., H.T., M.S., and E.C.G. performed the research. J.U., H.B.N., J.K.H., H.T., M.S., T.W., E.C.G. and S.M.S. analyzed various parts of the data and contributed to the writing of the paper.

DISCLOSURE: S.M.S. is a co-founder of Axerion Therapeutics, seeking to develop NgR-and PrP-based therapeutics.

affinity binding site for Aβ[5]. Binding of Aβo to PrP^C has been confirmed by in vivo and in vitro studies[6–10].

The contribution of Aβo/PrP^C complexes to AD models has been examined. Certain phenotypes occur in the absence of PrP^C[7,9,11,12]. In other paradigms, PrP^C is essential for Aβo-induced cell death and impaired synaptic plasticity, as well as AD transgene-induced spatial memory deficits, synapse loss, serotonin axon degeneration and early death[5,10,13–20]. Critically, human AD brain-derived extracts require PrP^C to suppress hippocampal long-term potentiation (LTP)[10,16]. Treatment of aged APPswe/PSen1-M146L mice with anti-PrP^C antibody reverses memory deficits and restores synaptic density[14]. Despite evidence that PrP^C binds Aβo and contributes pathogenically, signal transduction downstream of Aβo/PrP^C remains undefined.

Alterations in NMDA receptor (NMDA-R) function contribute to AD pathogenesis[21–23]. Therefore, Aβo/PrP^C complexes are predicted to modify NMDA-R function. Here, we examined the connection of Aβ/PrP^C signal transduction to NMDA-R dysfunction. We focused on Fyn kinase for several reasons. Both Fyn and PrP^C localize to lipid rafts, and clustering of PrP^C is reported to activate Fyn in cell lines[24–26]. Moreover, PrP^C loss-of-function in zebrafish is mimicked by reduced Fyn and rescued by increasing Fyn activation[27], while mutant PrP^C-induced degeneration in worm requires Fyn[28]. With regard to synapses, Fyn is localized to the post-synaptic density (PSD)[29], plays a critical role in LTP[30], and phosphorylates the NMDA-R subunits, NR2A/B[29,31]. Of relevance to AD, transgenic models are exacerbated by Fyn overexpression and ameliorated by Fyn deletion[32].

We show that PrP^C is enriched in the PSD, that Aβo binding to PrP^C activates Fyn, and that human AD brain-derived Aβ stimulates PrP^C signaling. This Fyn pathway leads to NR2B phosphorylation and altered NMDA-R localization, with destabilization of dendritic spines. A PrP^C-dependent pathway is required for seizures in AD transgenic mice, providing a basis for the rescue of survival by PrP^C deletion.

ON-LINE METHODS

Mice

WT, *Prnp*$^{-/-}$, APP/PSen and APP/PSen *Prnp*$^{-/-}$ mice on the C57B6/J background were as described[13]. *Fyn*$^{-/-}$ mice[51] were obtained from Jackson Laboratories. Both males and females were used in approximately equal numbers, and none excluded. All experiments were approved by the Institutional Animal Care and Use Committee.

Aβ peptide

Aβ42 oligomer, monomer and fibrillary preparations have been characterized[5]. Concentrations are in monomer equivalents. Oligomeric preparations with 1 μM total Aβ42 peptide contain about 10 nM oligomeric species[5].

Recombinant human PrP(23–111)

PrP(23–111) protein was produced by modification of previous procedures[52]. DNA encoding aa 23–111 of human PrP^C was cloned into pRSETA vector with an N-terminal extension encoding a hexa-histidine tag and thrombin cleavage site. Plasmid-transformed BL21(DE3) *E. coli* (Agilent) were cultured overnight without induction, and then diluted 1:100 in ZYM-5052 auto-inducing medium and grown for 16 h at 37C. Bacteria were lysed in Buffer G (6M Guanidine HCl, 100 mM Na_2HPO_4, 10 mM Tris-HCl, pH8) and then centrifuged at 100,000 × *g* for 1 h. The supernatant was applied to Ni-NTA resin. To refold bound protein, a 20–100% stepwise gradient of Buffer B (100 mM Na_2HPO_4, 10 mM Tris-HCl, 10 mM Imidazole, pH 8) in Buffer G was applied. After washing the resin, bound protein was eluted with 100 mM Na_2HPO_4, 10 mM Tris-HCl, 500 mM Imidazole, pH 5.8 and dyalized against 10 mM Na_2HPO_4 pH 5.8 and then against water. Final yields were 30–40 mg of protein per L of culture. Protein was stable at 4C for >2 months.

Generation of PrP^C and Fyn stable cell lines

PrP^C-expressing CV1 cells were isolated by clonal selection of a co-transfected Neo resistance gene in G418. A clone with PrP^C immunblot levels comparable to brain was propagated as SCA-7. Recombinant lentiviral particles expressing Fyn (pLEX-JRed, Open Biosystems) were transduced into CV-1 and SCA-7 cells. Cells stably expressing Fyn were selected with puromycin and confirmed by anti-Fyn immnuoblot. Cells were maintained in 25 μg/ml puromycin.

Cell line cultures and preparation of cell lysates

HEK293, CV-1 and Neuro-2A cells were rinsed with ice-cold PBS and solubilized in 20 mM Tris, pH 7.4, 1.0% Triton X-100, 0.1% SDS, 150 mM NaCl, 10% glycerol, complete protease inhibitor cocktail (Roche), phosphatase inhibitor (Roche). To separate cell lysates into soluble (S) and insoluble (I) fraction, material centrifuged at 20,000 × *g* for 20 min at 4C. Supernatants from the initial fractionation were saved as S fraction. The pellets were washed once with PBS before re-extraction with 2% SDS as I fraction.

Primary neuronal cultures

Rat E18 and mouse E17 cortical neurons were cultured for 21 days in Neurobasal-A media with B-27, 0.5 mM L-glutamine, penicillin and streptomycin (all from Invitrogen) on plates coated with poly-L-lysine.

Immunoblots

Protein was electrophoresed through 4–20% tris-glycine or 10–20% tris-tricine gels (Bio-Rad), transferred to nitrocellulose membranes (Bio-Rad) and blocked (Rockland MB-070-010). Membranes were incubated overnight 4C with primary antibodies: 6D11 (Covance 39810-500, 1:1000), anti-phospho-SFK (Cell Signaling Technology #2101, 1:1000), anti-Fyn (Cell Signaling Technology #4023, 1:1000), anti-Src (Cell Signaling Technology #2110, 1:1000), anti-Lyn (Santa Cruz Biotechnology sc-28790, 1:1000), anti-c-Yes (Santa Cruz Biotechnology sc-28883, 1:1000) anti-actin (Sigma-Aldrich A2066, 1:10000), anti-Myc (SIGMA C3956 1:1000), anti-GAPDH (Sigma-Aldrich G8795,

1:20000), anti-phospho-NR2B (pTyr1472) (SIGMA M2442, 1:1000), anti-NR2B (BD Transduction Laboratories #610416, 1:500), anti-PSD95 (Cell Signaling Technology #2507, 1:1000), anti-Synaptophysin (Cell Signaling Technology #4329, 1:1000), 6E10 (Covance SIG-39300 1:1000), 82E1 (IBL 1:100), anti-cleaved caspase-3 (Cell Signaling Technology #9661), anti-caspase-3 (Cell Signaling Technology #9665), anti-β amyloid (Cell Signaling Technology #2454, 1:1000). Secondary antibodies were then applied for 1 h at RT (Odyssey goat or donkey anti-mouse or anti-rabbit IRDye 680 or 800) and visualized with a Licor Odyssey system.

Immunoprecipitation

One μg of antibody was incubated overnight at 4C with 1 mg lysate protein. Thirty microliter of a 1:1 suspension of protein A-Sepharose (Amersham) was then incubated with sample for 2 h at 4C. The resin was washed, and immunocomplexes were resolved by SDS-PAGE and immunoblotted.

Immunocytochemistry

CV1-derived cells were fixed with formaldehyde and permeabilized with TritonX-100. Slides were blocked, and incubated at 4C with anti-phospho-SFK (1:100 dilution) and anti-PrP^C (6D11, Covance, 1:300 dilution). Alexa-Fluor-488 goat anti-mouse or Alexa-Fluor-568 goat anti-rabbit antibodies were used to detect bound antibodies.

Dissociated hippocampal neurons were prepared from E17-E18 C57BL/6 mice. At 21DIV, cultures were fixed in paraformaldehyde, permeabilized and blocked. Immunostaining was performed with antibodies against PrP^C (6D11, Covance, 1:100 dilution) and PSD-95 (Invitrogen #51–6900, 1:100 dilution) followed by Alexa-Fluor secondary antibodies. Images were acquired on a Zeiss (Oberkochen, Germany) LSM 510 META laser scanning confocal microscope using 63× water objective, with channels scanned separately and a pinhole set to 1.1 μm.

LDH release

LDH release into culture medium was measured with the Cytotoxicity Detection Kit (Roche). Total LDH was determined by lysing all cells with 2% TritonX-100, and experimental values expressed as percentage of total LDH. Absorbance was measured at 490 nm using a VictorX3 Multilabel Plate Reader (PerkinElmer).

MTT assay

Cell viability was monitored by the conversion of 3(4,5-dimethythiazozyl-2)-2,5 diphenyl tetrazolium bromide to colored formazan product (MTT; Roche). MTT labeling reagent (final concentration 0.5 mg/ml) was added to neurons and incubated for 4 h at 37C. Solubilization solution was added plates were incubated for 16 h at 37C. Colored formazan products were detected as absorbance at 550 nm in a VictorX3 Multilabel Plate Reader.

Cell surface biotinylation

Rat E18 and mouse E17 cortical neurons at 21DIV were untreated or treated with Aβo for various times, placed on ice and rinsed in cold PBS. Then, neurons were incubated with 1.5

mg/ml sulfo-NHS-LC-biotin (Thermo Scientific) in PBS for 30 min at 4C. Cells were rinsed to remove unbound biotin, and extracted with 1% TritonX-100, 0.1% SDS, complete protease inhibitor cocktail (Roche), phosphatase inhibitor (Roche). Biotinylated proteins were isolated with NeutrAvidin agarose (Pierce), separated by SDS-PAGE, and analyzed by immunoblotting.

NMDA-R trafficking

WT or *Prnp*$^{-/-}$ 14DIV cortical neurons were transfected with expression vector or NR2B-GFP (kindly provided by Dr. Yan, State University of New York[39]) using calcium-phosphate (Clontech). After 3 d, neurons were treated with 0–1 μM Aβo for 0–60 min. Neurons were placed on ice, and then incubated with Alexa Fluor 555-conjugated anti-GFP antibody (Molecular Probes, A31851) for 30 min. After three washes with PBS, the cells were fixed with 4% paraformaldehyde/4% sucrose in PBS for 15 m, and then washed 3 times with PBS. Images were acquired on a Zeiss LSM 510 META laser scanning confocal microscope with 63X objective, as above. The relative intensity (Surface/Total) normalized to the untreated condition was measured by MATLAB software. Values were collected from at least 4 fields in each culture condition.

Subcellular Fractionation of Brain Tissue

Rat forebrains were homogenized in ice-cold 5 mM NaHEPES, pH7.4, 1 mM $MgCl_2$, 0.5 mM $CaCl_2$, complete protease inhibitor cocktail (Roche), phosphatase inhibitor (Roche) with a glass/Teflon pestel. Extract was spun at 1400 × *g* for 10 min. Supernatant (S1) was centrifuged at 13,800 × g for 10 min to collect the pellet (P2). P2 was resuspended in Buffer B (0.32 M sucrose, 6 mM TrisHCl, pH 8.0, complete protease inhibitor cocktail (Roche), phosphatase inhibitor (Roche)). The P2 suspension was loaded onto a discontinuous sucrose gradient (0.85 M/ 1 M/ 1.15 M sucrose solution in 6 mM TrisHCl, pH 8.0), followed by centrifugation for 2 h at 82,500 × *g*. The synaptosome fraction between 1 M and 1.15 M sucrose was collected and adjusted to 4 ml with Buffer B. Equal volume of 6 mM TrisHCl, pH 8.1, and 1 % Triton X-100 was added and incubated for 15 min. The suspension was spun at 32,800 × *g* for 20 min. The resulting pellet was extracted again with 6 mM TrisHCl, pH 8.1 and 0.5 % Triton X-100 for 15 min, and spun again at 201,000 × *g* for 1h. Resulting pellet was analyzed as the PSD.

Human Brain Fractionation

Fresh-frozen post-mortem human pre-frontal cortex from the brains of AD patients or Control subjects were obtained from pre-existing collections, as approved by Yale Institutional Review Board. Clinical diagnoses were confirmed histologically by examination of adjacent tissue in paraffin sections for abundant Aβ plaques and neurofibrillary tangles, Braak stage VI. Demographic and case details are provided in Suppl. Fig. S5d. One g tissue was homogenized in 5 ml of 25 mM Tris pH 7.4; 100 mM NaCl; protease inhibitor cocktail, Roche Diagnostics 11836170001, using a polytron. Particulate components were removed after centrifugation at 175,000 × *g* for 30 min.

For PrP-Fc affinity resin absorption, TBS-soluble extracts were cleared overnight at 4°C with Protein A sepharose beads (GE 71-5002-73 AI), followed by 2 hours clearance with the

same beads crosslinked to human Fc (Jackson Immunoresearch 009-000-008). Equal volumes of cleared extract were incubated 4 h at 4°C with the same beads covalently crosslinked with either human Fc or recombinant human PrP-Fc. The unbound material was utilized for activity assays.

Assay of PrP^C-Interacting Aβ Species in Brain Samples

To prepare capture plates, 20 μl/well of 0 or 100 nM human recombinant PrP(23–111) in 30 mM Na_2CO_3, 80 mM NaHCO3, pH 9.6 was added to 384-well Black MaxiSorp ELISA plates (Thermo Scientific). After 2 h at 23C, plates were washed with PBS-T and blocked with 5% BSA in PBS-T (100 μl/well) overnight at 4C. After washing again, samples (50 μl) were applied and incubated for 1h at 23C. All the samples included added BSA at 0.5%. The plates were then washed, and 20 μl/well of rabbit anti-amyloid beta antibody (#2454, Cell Signaling Technology, 1:1000 dilution in PBS-T, 0.5%BSA) was added for 1h. After another wash, plates were incubated with 20 μl/well of biotinylated donkey anti-rabbit antibody (Jackson Immunoresearch, 1:1000 in PBS-T, 0.5%BSA) for 30 minutes, washed 3X with PBS-T and then incubated with 20 μl of Europium-conjugated streptavidin, 1:1000 in DELFIA Assay Buffer (Perkin Elmer). After a final 4X PBS-T wash, 20 μl of DELFIA Enhancement Solution (Perkin Elmer) was added to the wells and time-resolved Europium fluorescence was measured using Victor 3V plate reader (Perkin Elmer). Background fluorescence values from uncoated wells were subtracted from the corresponding values of PrP^C-coated wells.

For PrP(23–111) depletion of Aβ from AD brain TBS-soluble extracts, samples were incubated with PrP(23–111)-coated or uncoated control wells in 96-well BSA-blocked MaxiSorp plates (Nunc 80040LE 0903) for 3 h at 23C. Unbound material was recovered for ELISA. The plates were washed 4 times with PBS-T, and bound Aβ was eluted from PrP(23–111) using 30 μl/well of 10M urea. The original and recovered extracts, as well as the urea elutions, were assayed for Aβ42 using a commercially available kit (Invitrogen KHB3441). Elution fractions were diluted to 1M urea prior to ELISA.

Imaging of Dendritic Spine Stability

Hippocampi were dissected from E17–19 mouse embryos and digested with papain (37C; 5% CO2 for 30 min), and then washed with 1X HBSS. The neurons were transfected with myristoyl-EGFP expression vector using an Amaxa Nucleofector, and plated on poly-D-lysine-coated (100 μg/ml) glass at 100,000 cells/well in 8 well plates (Lab-Tek Chambered Coverslip 155411). WT controls were plated on half of the 8-well dish and either *Fyn*$^{-/-}$ or *Prnp*$^{-/-}$ neurons on the other half of the 8-well dish. Culture medium was Neurobasal A supplemented with penicillin/streptomycin, 1 mM Na-pyruvate, 2 mM GlutaMax, and B27 supplement.

Between 19–23DIV, hippocampal neurons were observed with a 100X objective on a Nikon Eclipse Ti Spinning Disk Confocal Microscope using a 488 laser. Approximately 25 fixed locations per 8-well dish were imaged on an automated stage every 15 min for 6 h in a 10 μm Z-stack at 0.1 μm intervals. For the first h, neurons were untreated. After 1 h, neurons

were treated with 500 nM Aβo or F12 vehicle and imaged for 5 h. In some experiments, 50 μM AP5 or vehicle were added immediately before Aβo.

Dendritic spine persistence or creation was assessed in consecutive images of the dendritic segments using ImageJ software without knowledge of genotype or treatment. For each embryo, at least 4 segments with >30 spines were monitored, and statistics were calculated based on variablility between separate embryo cultures. Rare images showed dendritic segments with widespread blebbing and retraction; these were excluded from the analysis.

Cellular Aβ oligomer binding assay

Aβo binding was performed as described[5] with slight modifications. Briefly, transfected COS7 cells were treated with biotinylated Aβo at 4C for 1 h. After washing, cells were fixed, incubated at 65C for 2 h, and incubated with alkaline-phosphatase-conjugated neutravidin. Bound phosphatase was visualized by 5-bromo-4-chloro-3-indolyl phosphate/nitro blue tetrazolium reaction and quantified with ImageJ[5].

Measurement of intracellular calcium

Cortical neurons (21DIV) from WT, *Prnp*$^{-/-}$ or *Fyn*$^{-/-}$ mouse embryos were incubated in 96 well plates and treated with 0–1 μM Aβo for 0–60 min plus a calcium dye (FLIPR Calcium 4 assay kit, Molecular Devices). Plate fluorescence (λ_{ex} = 485 nm, λ_{em} = 535 nm) was monitored in a VictorX3 Multilabel Plate Reader (PerkinElmer) with or without 50 μM NMDA, 100 μM glutamate or 500 nM ionomycin.

EEG surgeries and analysis

We studied 9–10 month old mice of the following genotypes: WT (C57B6/J) (n=11), *Prnp*$^{-/-}$ (n=11), APP/PSen (n=10), and APP/PSen *Prnp*$^{-/-}$ (n=12). Mice were anesthetized with isoflurane, and mounted in a stereotaxic frame (Kopf). A midline incision was made, and 2 bilateral burr holes were drilled anterolateral and posterolateral to bregma. Four pre-soldered intracranial screw electrodes (Pinnacle Technology #8403) were inserted, and secured with dental cement (A-M Systems #526000). Electrode wires were soldered to a 6-pin surface mount connector (Pinnacle Technology #8235-SM). Mice were allowed to recover for 7 d prior to EEG.

Mice were recorded using video-EEG monitoring (Pinnacle Systems #8200-K1-SE3, #8236). EEGs were sampled at 400HZ with 100X preamplifier gain. Each mouse underwent 72 h of continuous recording. EEG traces were scored manually by an investigator unaware of genotype. A seizure was defined as the abrupt onset of evolving spike-and-wave discharge lasting >5 s, followed by a period of post-ictal attenuation of cerebral rhythms. The recorded seizures were each 20–60 s in duration. There was no requirement for bilateral involvement, but all recorded seizures were generalized. Each seizure was correlated with the video recording and each was accompanied by convulsive behavior. Four of ten APP-PSen had ≥1 seizure over 72 h. Two mice had 1 seizure in this period, the third mouse had 1 seizure per d, and the 4th mouse had an average of 1–2 seizures per d (a total of 5 in 3 d).

There were also single spikes and 3–5 s spike wave discharges that were not analyzed here. Subjectively, spike wave discharges were specific to APP/PSen mice, and greatly reduced by *Prnp* deletion.

Statistical analyses

Statistical comparisons included one-way ANOVA and Repeated Measures ANOVA with post-hoc Tukey pairwise comparisons, as specified in the Figure Legends, using SPSS or Prism statistical software. Survival data were analyzed with the logrank test (Mantel-Cox) with SPSS software.

RESULTS

Prion Protein is Enriched in Post-Synaptic Densities

Aβo binding sites show post-synaptic dendritic localization[5,22,33]. To the extent that PrP^C is relevant to Aβo-driven pathology, it may be concentrated in similar regions. Our initial studies documented co-localization between Aβo binding and PrP^C, but did not characterize sites of PrP^C enrichment[5].

The PSD is distinct ultrastructurally and biochemically. Proteomic analyses of PSDs by mass spectrometry have revealed PrP^C as a component[34]. To define PrP^C enrichment in the PSD, we performed immunoblots on various subcellular fractions (Fig. 1a, b). PrP^C is enriched in synaptosomal fractions. Isolation of the PSD from synaptosomes segregates the PSD-95 marker protein fully to the PSD and synaptophysin to the detergent extractable fraction. Substantial amounts of PrP^C co-fractionate with PSD-95, yielding five-fold PrP^C enrichment in PSD relative to initial homogenate. Fyn kinase is enriched three-fold in PSDs. We also observed substantial colocalization of PSD-95 with PrP^C immunoreactivity in hippocampal cultures (Fig. 1c). Thus, PrP^C is present in the PSD where it may mediate effects of Aβo.

Aβo Binding to PrP^C Generates Fyn Kinase Activation

The non-receptor tyrosine kinase Fyn is a candidate mediator of signal transduction from an Aβo/PrP^C complex for the reasons introduced above. It is possible to monitor the activation of Src family kinases (SFK) by phospho-specific epitopes. We examined cultures for SFK activation after exposure to Aβ species for 15 minutes (Fig. 2, Suppl. Figs. S1–4). Wild type cortical neurons at 21 days in vitro (DIV) increase pY416-Fyn (SFK) in response to Aβo (Fig. 2a, c). This antibody detects pY416 in several SFKs, but kinase-specific immunoprecipitations demonstrate that PrP^C-dependent activation is Fyn-specific (Suppl. Fig. S1a). Fyn activation is oligomer-specific, not being observed with monomeric Aβ (Fig. 2c, Suppl. Fig. 1b) or fibrillary Aβ (Suppl. Fig. S1c,d).

We asked whether PrP^C is required for the Aβo-induced Fyn activation. Previously, we showed that Aβo binding to PrP^C is blocked by anti-PrP^C 6D11 antibody[5]. This antibody also prevents Fyn activation by Aβo (Fig. 2a, c). Most importantly, in $Prnp^{-/-}$ cultures, activation of Fyn by Aβo is eliminated (Fig. 2b, c). Absence of Fyn signaling in $Prnp^{-/-}$ neurons is specific for Aβo, since Reelin-induced Fyn activation is preserved (Fig. 2d, e).

Thus, while PrP^C accounts for ~50% of Aβo binding sites[5,33], it accounts fully for Fyn signaling.

We also verified Aβo-induced PrP^C-dependent Fyn activation in cell lines. Stably transfected CV1 cells expressing PrP^C (Sca-7), Fyn or both were generated (Suppl. Fig. S2a). PrP^C protein in parental CV1 cells is <5% that in brain, and the level in PrP^C expressors is 50–100% of brain (not shown). Aβo enhances pY-416-SFK level 2-fold exclusively in the PrP^C/Fyn cells (Suppl. Fig. S2a, b). In N2A neuroblastoma, similar PrP^C-dependent, Aβo-induced Fyn activation is observed in detergent-insoluble subcellular fractions (Suppl. Fig. S2c, d), though activation is not detected in HEK293T cells. We conclude that Aβo/PrP^C complexes activate Fyn in many cells.

A marker of Aβo-induced PrP^C/Fyn signaling is physical proximity of the proteins. In untreated CV-1 or HEK cells, a proportion of Fyn co-immunoprecipitates with PrP^C (Suppl. Fig. S3a, b). Association is increased by Aβo treatment. An Aβo-induced complex can also be observed immunohistologically (SCA-7/Fyn cells, Suppl. Fig. S3c). At baseline, CV-1 cells expressing PrP^C and Fyn show plasma membrane PrP^C and diffuse Fyn staining with limited overlap. After Aβo, PrP^C immunoreactivity is concentrated at the cell periphery in ruffles together with bound Aβo, with total Fyn, and with activated Fyn.

Cell-bound Aβo[26], PrP^C and Fyn are known to localize to lipid rafts. When rafts are disrupted by pretreatment of cultures with methyl-β-cyclodextrin (MBCD), Aβo activation of Fyn is absent from primary neurons (Fig. 2f, g), from CV-1 cells (Suppl. Fig. S4a) and from neuroblastoma cells (Suppl. Fig. S4b). The Aβo induced-enhancement of PrP^C/Fyn co-immunprecipitation is absent after MBCD preincubation (Suppl. Fig. S4c). Phosphoinositide-specific phospholipase C (PI-PLC) releases GPI-anchored PrP^C into the medium, and no Aβo signaling occurs in neurons (Fig. 2f, g) or cell lines (Suppl. Fig. S4a, b). Thus, GPI-anchored PrP^C and intact lipid rafts are required for Aβo signaling to Fyn.

Aβo may activate PrP^C/Fyn signaling by altered PrP^C clustering or by induced PrP^C conformations or by differential association with other proteins. To examine PrP^C clustering, we treated primary neurons with anti-PrP^C antibodies (6D11 or SAF32), as described for other cells[24,25,35]. Neither bivalent nor clustered anti-PrP^C activates Fyn in primary neurons (Fig. 2h, i). Thus, PrP^C clustering alone is not sufficient for the Aβo activation of Fyn in neuronal lipid rafts.

Human AD Brain Contains PrP^C Interacting Aβ Species

Aβo have been prepared from multiple sources including synthetic peptide, transgenic mouse brain, transfected cell lines and human AD brain[1–4]. It is critical to evaluate human AD brain-derived Aβo of greatest relevance for pathophysiology. Importantly, human AD brain-derived Aβo require PrP^C to suppress LTP[10,16]. Therefore, we assessed PrP^C-interacting Aβo from human AD tissue for Fyn activation (Fig. 3)

We developed a sensitive assay for the detection of Aβ species interacting with PrP^C (Fig. 3a). The 23–111 Aβ-interacting domain of PrP^C was purified from recombinant *E. coli* and immobilized in microtiter plates. Specimens containing Aβo were added, and bound Aβ was

detected with anti-Aβ antibodies. Detection of PrP^C-bound Aβo was robust with N-terminally directed Aβ antibodies, polyclonal 2454 and monoclonal 82E1 (Suppl. Fig. S5a), or with NU-4 anti-oligomer antibody (not shown), but not with C-terminally directed antibodies, including AB5306 (Suppl. Fig. S5a). This may be due to inaccessibility of the Aβ C-terminus in oligomeric assemblies under native conditions. Using purified Aβo, the assay has a linear range from 20 pg to 14,000 pg (Fig. 3a). The specificity for oligomeric Aβ over monomeric Aβ or fibrillary Aβ exceeds 30-fold (Fig. 3a).

We assessed PrP^C-interacting Aβ species in brain TBS homogenates cleared by ultracentrifugation. PrP^C-interacting Aβ is detected in transgenic APP/PSen mouse brain, but not in WT brain (using synthetic Aβo as standard, 394±72 (transgenic, n=9 brains) *versus* <15 (WT, n=7) ng Aβ/g brain, mean ± sem, $P<0.001$, ANOVA, F=28.48; df=1). We measured PrP^C-interacting Aβo in TBS-soluble cortical extracts from a cohort of autopsy-confirmed AD cases versus Controls. The average level in Control brains is below the detection limit, while AD samples contain 20.8+2.6 ng Aβ/g brain (Fig. 3b, mean ± sem, $P<0.001$, AD versus Control). This value suggests that a substantial proportion of Aβ in TBS-soluble extracts of AD brain interacts with PrP^C. ELISA measurement demonstrates that ~50% of Aβ42 immunoreactivity in TBS-soluble AD extract absorbs to PrP-coated wells (Suppl. Fig. 5b). Urea elution recovers ELISA-detectable Aβ42 selectively from PrP(23–111) wells exposed to AD extracts (Suppl. Fig. 5c). Urea allows >100% recovery of initial Aβ42 ELISA signal (Suppl. Fig. 5b, 5c), likely due to denaturation of secondary structure in Aβ or associated proteins, which otherwise limit detection.

Having detected PrP^C-interacting Aβ in human AD brain, we sought to determine whether these assemblies activate neuronal Fyn (Fig. 3c–e). AD brain extracts at 6 μg protein/ml stimulate Fyn activation in mouse cortical cultures, but Control brain extracts do not (Fig. 3c, d, $P<0.05$). To assess whether this actvation is due to PrP-interacting species, we preabsorbed human TBS brain extracts with PrP^C-Fc affinity resin. PrP^C-Fc resin, but not Fc control resin, prevents Fyn activation (Fig. 3c, e). The Aβ dependence of Fyn activation was assessed with anti-Aβ 82E1 antibody; abrogation is observed (Fig. 3c, e). As for synthetic Aβo stimulation of Fyn above, the signaling induced by AD TBS extract is absent in $Prnp^{-/-}$ cells, or in cells pretreated with 6D11 anti-PrP^C antibody (Fig. 3c, e). Moreover, the level of PrP^C-interacting Aβ species in human brain extracts correlates with the level of Fyn activation (Fig. 3f). Thus, TBS-soluble Aβ derived from human AD stimulates neuronal Fyn via PrP^C.

NMDA-R Subunits Phosphorylated by Aβ/PrP/Fyn Signaling

NMDA-Rs play a key role in synaptic plasticity and AD. Intracellular segments of NR2A and NR2B subunits contain tyrosine residues phosphorylated by SFKs[36]. Thus, Aβo/PrP^C-mediated Fyn activation may be directed to NMDA-R. We examined total and pY-1472 NR2B levels in neuroblastoma cells expressing Fyn, PrP^C and NR2B after exposure to Aβo (Suppl. Fig. S6a). Selectively in Fyn-overexpressing cells, Aβo increases pY-1472 NR2B. This increase is blocked by 6D11 anti-PrP^C antibody. Next, we studied endogenous proteins in cortical cultures exposed to Aβo (Fig. 4a, b). Over 20 minutes, Aβo induces a dose-dependent 5-fold increase in pY-1472 NR2B. This effect is specific for the oligomeric Aβ,

since fresh Aβ has no effect (not shown). Aβo-induced NR2B phosphorylation is eliminated in *Prnp*$^{-/-}$ cultures (Fig. 4a, b), in *Fyn*$^{-/-}$ cultures (Suppl. Fig. S7b), and by 6D11 anti-PrP^{C} antibody (Fig. 4a, b). Thus, Aβo-induced phosphorylation of Y1472 in NR2B is a PrP^{C}/Fyn-mediated signaling event. Moreover, the roles of PrP^{C} and Fyn are gene-dose-dependent, being reduced in heterozygous neurons (Suppl. Fig. S7a, S7c).

During the first 15 minutes with Aβo, NR2B phosphorylation is enhanced, but after 1–3 hours phosphorylation is suppressed (Fig. 4c, d). Aβo is known to increase STEP tyrosine phosphatase[23,37]. Since STEP and Fyn counteract one another, we compared the time course of these events relative to NR2B phosphorylation (Fig. 4c, d). At the onset of Aβo action, Fyn is activated and pY-1472-NR2B is increased with no change in STEP. Later, STEP increases while Fyn returns to baseline with a net decrease in NR2B phosphorylation. Thus, a biphasic effect of Aβo on NR2B is triggered by PrP^{C} engagement.

Surface NMDA-R and Calcium Signaling Induced by Aβ/PrP/Fyn

Phosphorylation of NR2B at Y1472 is known to reduce AP-2 mediated endocytosis[38]. We examined the extent to which NR2B is accessible at the cell surface versus being sequestered intracellularly, using cell surface biotinylation (Fig. 5a–d). In concert with the NR2B-pY-1472 increase, biotinylated NR2B increases shortly after Aβo exposure (Fig. 5a, d). There is no change in total NR2B. The increase is transient, and is followed by suppression of surface NR2B below baseline, matching the late decrease in pY-1472-NR2B. Both the early and late surface NR2B response to Aβo require PrP^{C} and Fyn, as demonstrated by lack of response in *Prnp*$^{-/-}$, *Fyn*$^{-/-}$ and 6D11-treated cultures (Fig. 5a–d). The levels of PrP^{C} are limiting, with a substantial reduction in short-term Aβo-induced NR2B relocalization in *Prnp*$^{+/-}$ neurons (Suppl. Fig. S7d). The biochemical changes can be imaged using an extracellularly GFP-tagged NR2B[39]. The ratio of surface:total NR2B protein is detected by assessing the anti-GFP staining without permeablization versus the intrinsic GFP fluorescence (Fig. 5e, f). In WT neurons, Aβo triples this ratio at 15 minutes with a return to baseline by 60 minutes. There is no change in neurons lacking PrP^{C}.

Changing surface levels of NMDA-R are expected to mediate alterations in NMDA-induced calcium levels. We utilized a calcium-sensitive fluorescent dye to monitor intracellular calcium in cortical neurons. NMDA produces increased fluorescence signal microscopically (Supplemental Movie S1) or in microtiter wells (Fig. 5g). Pretreatment with Aβo for 15 minutes generates significantly increased NMDA-induced signal, as predicted. By 60 minutes, when NR2B receptors are dephosphorylated and internalized, NMDA-induced calcium signals are suppressed (Fig. 5g). In cortical neurons lacking PrP^{C}, Aβo does not alter NMDA responsiveness (Fig. 5g). The Aβ effect was oligomer-specific, since neither Aβ monomers nor Aβ fibrils alter NMDA responses (Suppl. Fig. S8d). Bath application of glutamate produces elevations of intracellular calcium that are mediated by NMDA receptors and by other channels. One hour pretreatment with Aβo suppresses glutamate responses in WT, but not in *Prnp*$^{-/-}$ or *Fyn*$^{-/-}$ neurons (Suppl. Fig. S8a–c). Thus, Aβo-induced, PrP^{C}-mediated alterations in NMDA-R create transient increases and then decreases in neuronal calcium.

We considered whether the transient increase in surface NR2B might lead to a brief period of excitotoxicity. We first examined N2A cells with and without overexpression of Fyn and PrP^C. Combined expression of Fyn plus PrP^C substantially increases the release of cellular LDH induced by 90-minute exposure to Aβo (Suppl. Fig. S6b). To explore a role for endogenous PrP^C and Fyn in Aβo neuronal toxicity, we used primary cortical cultures. Brief exposure to Aβo reduces cell viability, with a release of 10% of cellular LDH (Fig. 5h, Suppl. Fig. S8e). A decrease in MTT reduction is not detectable, being within the range of variability of the assay (Suppl. Fig. S9a). When Aβo exposure is extended to 72 hours, no further LDH release is observed (Suppl. Fig. S9b), indicating that this cell toxicity occurs largely during the initial 90 min of Aβo exposure, when surface NR2B is increased.

To determine whether the correlation of acute Aβo cell toxicity with surface NR2B and Aβ/PrP/Fyn signaling is functional, we examined the effects of antibody and genetic blockade. Anti-PrP^C 6D11 antibody pretreatment prevents the Aβo-induced LDH release (Fig. 5h). A requirement for PrP^C in Aβo-induced neuronal cell death matches recent reports[15,20]. Genetic deletion of either Fyn or PrP^C expression rescues neurons from Aβo (Fig. 5h). Heterozygosity for null alleles of *Prnp* or *Fyn* significantly reduces LDH release (Suppl. Fig. S7e). For transheterozygous $Prnp^{+/-}$, $Fyn^{+/-}$ neurons, there is no detectable Aβo-induced LDH release during 90 minutes (Suppl. Fig. S7e). The toxicity depends primarily on NMDA-R since it is reduced by AP5, and on NR2B-containing receptors since ifenprodil suppresses LDH release (Fig. 5i). Consistent with an excitoxic, non-apoptotic cell toxicity, there was no increase in activated caspase 3 (Suppl. Fig. S9c, S9d). Thus, Aβo requires PrP^C to induce Fyn activation and subsequent NR2B phosphorylation. This phosphorylation is associated with transient increase in NR2B at the cell surface with consequent excitotoxicity.

Aβo Destabilization of Dendritic Spines Requires PrP/Fyn

A hallmark of AD is synaptic loss[40]. In vitro studies have described dendritic spine loss after acute Aβo exposure[3,21,22]. We sought to assess whether PrP^C and Fyn are involved. To provide a robust measure for fractional loss, we repeatedly imaged the same dendritic segments expressing membrane-tethered EGFP over 6 hours (Fig. 6a, Supplemental Movie S2). Under control conditions, dendritic spines are stable, with <2% gains or losses. Aβo increases spine loss, without significant alteration of spine gain. Over 5 hours, 10–15% of spines are lost with Aβo, while adjacent spines are morphologically stable (Fig. 6a, c). The time course is gradual after an initial lag (Fig. 6b). Although loss is increased five-fold by Aβo, loss remains minor compared to the variability of spine density, emphasizing the need for time-lapse imaging.

To assess the roles of PrP^C and Fyn in Aβo-induced spine loss, neurons were cultured from embryos homozygous for null alleles (Fig. 6a, c). Spine destabilization by Aβo is eliminated in $Prnp^{-/-}$ and $Fyn^{-/-}$ neurons. Thus, Aβo-induced spine loss requires both PrP^C and Fyn. We also tested whether Aβo-induced spine loss requires NMDA-R. As shown in previous studies with human AD brain derived species[3], the NMDA antagonist AP5 blocks dendritic spine loss by Aβo (Fig. 6c).

Seizures in AD Transgenic Mice are Prevented by *Prnp* Loss

Epileptiform discharges have been observed in transgenic mouse models of AD and seizures are more common in AD[41]. We hypothesized that network instability may derive from Aβ/PrP/Fyn-induced alterations in synapses. We examined epileptiform discharges of >5 sec in APPswe/PSen1ΔE9 transgenic mice with or without PrP^C expression at 9–10 months of age (Fig. 7a, b). After implantation of intracranial electrodes, continuous video plus EEG records were monitored for 72 hours. Consistent with previous studies[42], 40% of APP/PSen transgenic mice had at least one electrographic seizure (Fig. 7b). The majority included an initiating spike, a 20s–60s run of high amplitude epileptiform activity and were followed by a post-ictal attenuation of cerebral rhythyms (Fig. 7a). At the video level, each of the electrographic seizures was accompanied by tonic posturing and myoclonus (Supplemental Movies 3, 4). The ictal period commonly includes locomotor hyperactivity, and the postictal period is marked by hypoactivity. None of the 12 APP/PSen transgenic lacking PrP^C exhibited an electrographic or behavioral seizure during 72 hours (Fig. 7b). Neither the WT nor *Prnp*$^{-/-}$ mice had electrographic abnormalities during similar monitoring, though single spikes were occasionally observed in all genotypes. Thus, the electrographic phenotype of this AD model requires PrP^C.

The seizure phenotype may account for the reduced survival of APP/PSen via status epilepticus, or Sudden Unexpected Death in Epilepsy (SUDEP). In the cohort studied here, reduced survival for the APP/PSen genotype is fully rescued by PrP^C loss (Fig. 7c), as in our previous separate analysis[13]. De facto, mice monitored by EEG are selected from the two-thirds of transgenic mice that escaped early death. Considering both phenotypes together, 70% of the APP/PSen mice suffered either early death or seizures, while <4% of the APP/PSen, *Prnp*$^{-/-}$ mice showed one of these phenotypes.

DISCUSSION

We delineate a Fyn signaling pathway activated by Aβo/PrP^C complexes. Pathophysiological relevance is supported by the binding of human AD-derived Aβo to PrP^C, the enrichment of PrP^C in PSDs, the PrP^C-dependence of Fyn activation by Aβo in neurons, and the requirement of both Fyn and PrP^C for Aβo-induced changes in NR2B. Short-term activation of this pathway increases in surface NMDA-R and excitotoxicity, followed by dendritic spine and surface receptor loss. The complete rescue of AD transgene mortality by PrP^C deletion is dramatic, and may be secondary to the PrP^C-dependence of epileptiform activity detected by EEG recording. Together, these data document a biochemical pathway downstream of Aβo/PrP^C complexes that has potential contributions to AD pathogenesis (Suppl. Fig. S10).

Different Aβ Oligomer Species and Mechanisms

Aβo derived from synthetic peptide, cell culture, transgenic brain and human AD brain have been analyzed in various functional and biochemical assays. The Aβ peptide can assume different oligomeric states, each distinct from monomer or fibrillary peptide. The resolution of oligomeric Aβ forms is not defined biophysically, though molecular weight and/or valency clearly differ between preparations. Variable outcomes in functional experiments

with different Aβo preparations may derive from uncharacterized variation between preparations[10]. Here, we demonstrate that Aβo from human AD brain interacts with PrP^C, confirming the pathological relevance of the studies. PrP^C-dependence for human AD brain extract suppression of LTP has been reported recently[10,16].

The ability of Aβo species to interact with PrP(23–111) distinguishes a subset of peptide with deleterious actions on neurons and synapses. The level of PrP^C-interacting Aβ species in AD brain TBS-soluble extracts is within the range of values from previous studies[43–45]. Measurements of Aβ after immunopreciptitation/immunblot of AD brain TBS-soluble extracts yielded values[43] very similar to the values reported here for PrP^C-interacting species. This raises the possibility that a substantial fraction of Aβ in human AD brain is capable of PrP(23–111) interaction. Further analysis of human samples for PrP^C-interacting Aβ species may provide a useful tool to follow disease status and/or treatment efficacy.

Post-Synaptic Action of Aβo/PrP^C Complexes

Synapse loss is amongst the most prominent and consistent aspects of AD[40]. Here, immunohistochemical localization and subcellular fractionation studies demonstrate that PrP^C is concentrated at synapses and enriched in PSD. These findings are consistent with several unbiased proteomic studies documenting PrP^C in PSD fractions[46,47] and PrP^C is included in a “Consensus PSD” data set[34]. PSD localization fits with a role for PrP^C in mediating local effects of Aβo on synaptic plasticity, dendritic spine retraction and synaptic loss. Indeed, our genetic analysis demonstrates that both PrP^C and Fyn are required for dendritic spine loss. Previous studies have demonstrated that chronic loss of synaptic markers in transgenic AD mice requires PrP^C[13,14]. However, another study found that Aβ-induced loss of dendritic spines in culture was PrP^C-independent12. The PrP^C-negative result may reflect differences in the Aβ preparation. In this regard, the observation that PrP^C-Fc recognizes AD-derived Aβ species, supports a disease relevance for PrP^C-dependent pathways.

Engagement of an Aβo/PrP^C/Fyn pathway increases NMDA-R phosphorylation and alters receptor localization. The biphasic effect on surface NMDA-R is coupled with short-term cell toxicity followed by a loss of surface receptor. Both acute augmentation and chronic suppression of NMDA responses by Aβo have been reported in various studies[18,21,48]. Future studies of GluR trafficking will delineate the sites of receptor relocalization within the neuron relative to synapes, as well as the timing of Aβo/PrP^C/Fyn induced changes in neurotransmission.

Fyn Activation by PrP^C

While PrP^C and Fyn are associated physically and Aβ engagement of PrP^C leads to Fyn activation, the two proteins are on different faces of the plasma membrane. PrP^C is extracellular while Fyn is intracellular, so that the two polypeptides cannot be in direct physical contact. Lipid rafts are crucial for signal transduction and cell-bound Aβo is known to localize to rafts in a Fyn-dependent manner[26]. It is possible that the coalescence of Aβo/PrP^C and Fyn in lipid rafts allows signaling without a transmembrane polypeptide

partner. However, it seems more plausible that there are one or more membrane-spanning partners that link the two proteins.

Previous reports have described PrP^C-dependent signaling in certain cells after antibody cross-linking[17,24,25]. We find that clustering of PrP^C with anti-PrP antibodies is not sufficient to induce Fyn activation as observed with Aβo in primary neurons. This suggests that PrP^C conformational changes occur when Aβo binds. The Aβo binding domain of PrP^C, aa 23–111, is thought to be natively disordered, so Aβo may stabilize a specific conformation of the protein leading to signal transduction through Fyn.

Although acute engagement of PrP^C by Aβo activates Fyn, in vivo levels of Fyn are similar in WT and AD transgenic mice[32]. This is likely related to secondary changes in the chronic state. The biphasic effect of Aβo on NMDA-R is consistent with compensatory dysregulation. In this regard, it is notable that the STEP phosphatase counteracts Fyn activation and STEP levels are induced in transgenic AD models and AD[32,37]. In culture, early PrP^C-dependent Fyn activation is required for the later loss of surface NMDA-R, which is correlated with STEP expression. Such compensation may play a crucial role in chronic AD pathophysiology after acute Aβo/PrP^C/Fyn engagement.

Fyn in PrP^C-Dependent and AD-Related Pathways

These studies suggest that Fyn plays a central role in coupling Aβo and PrP^C to changes in neuronal function. There are multiple lines of evidence linking Fyn kinase function to synapse plasticity and dysfunction in AD. Fyn is enriched in the PSD, and is known to phosphorylate NR2A and NR2B[29]. Mice with loss of Fyn function exhibit reduced LTP, while gain-of-function leads to enhanced LTP and seizures[30,49]. When Fyn mutants are crossed with APP transgenic mice, Fyn gain-of-function enhances AD-related phenotypes while Fyn loss-of-function ameliorates AD-related phenotypes[32]. Fyn is known to associate with Tau and recent data indicate that aberrant Fyn-Tau interactions sensitize synapses to glutamate excitoxicity[50]. PrP^C/Fyn signaling may couple Aβ and Tau pathologies.

The data here provide evidence that PrP^C and Fyn are essential for certain Aβo induced biochemistry and AD transgene-dependent phenotypes. Other signaling pathways participating in Aβ action include calcineurin, insulin receptors, autophagy, glutamate reuptake and Tau-directed kinases. The interdependence and epistatic relationships between these multiple pathways require further investigation.

Seizures and AD

Mice carrying human AD transgenes exhibit altered network activity and epileptiform discharges[41]. We confirmed a similar finding in APPswe/PSen1ΔE9 mice[42] and show that this phenotype is PrP^C-dependent and includes convulsive seizures. Single spikes without behavioral changes were not a reliable distinguisher between WT and APP/PSen transgenic phenotypes in our studies. Since Fyn gain-of-function reduces seizure thresholds[49], Aβo/PrP^C/Fyn signaling may explain abnormal EEG patterns. It has been suggested that epileptiform discharges explain early death in AD transgenic mice. The PrP^C-dependence of both epileptiform activity and early death provides indirect support for this hypothesis.

While seizure incidence has been reported to increase in AD, sudden death early in the disease is not typical. The relevance of EEG abnormalities to cognitive dysfunction in AD requires clinical correlation.

Conclusions

Previous work has demonstrated that Aβo bind to $PrP^{C5–10}$, and in a number of scenarios PrP^{C} is essential for the deleterious actions of $Aβo^{5,10,13–20}$. Here, we provide evidence for Fyn kinase signaling that links an Aβo/PrP^{C} complex in PSDs to changes in GluR function and dendritic spine anatomy. Importantly, Aβo from AD brain interact with PrP^{C}, so this complex may play a pathological role in human AD. Furthermore, Fyn provides a molecular link to Tau pathology and to epileptiform phenotypes. Future studies will examine the Aβo/PrP^{C}/Fyn pathway in multiple models of AD to validate its relevance for pathophysiology in different disease stages and manifestations.

Supplementary Material

Refer to Web version on PubMed Central for supplementary material.

ACKNOWLEDGMENTS

H.B.N. is an Ellison Medical Foundation AFAR Postdoctoral Fellow and S.M.S. is a member of the Kavli Institute for Neuroscience at Yale University. We acknowledge support from the National Institutes of Health (R01AG034924, R37NS033020, R01NS074319, P30DA018343), the Falk Medical Research Trust, and the Alzheimer's Association to S.M.S., and from the National Institutes of Health (R01NS47433, R01NS073502) to T.W.

REFERENCES

1. Lambert MP, et al. Diffusible, nonfibrillar ligands derived from Abeta1-42 are potent central nervous system neurotoxins. Proc Natl Acad Sci U S A. 1998; 95:6448–6453. [PubMed: 9600986]
2. Walsh DM, et al. Naturally secreted oligomers of amyloid beta protein potently inhibit hippocampal long-term potentiation in vivo. Nature. 2002; 416:535–539. [PubMed: 11932745]
3. Shankar GM, et al. Amyloid-beta protein dimers isolated directly from Alzheimer's brains impair synaptic plasticity and memory. Nat Med. 2008; 14:837–842. [PubMed: 18568035]
4. Lesne S, et al. A specific amyloid-beta protein assembly in the brain impairs memory. Nature. 2006; 440:352–357. [PubMed: 16541076]
5. Lauren J, Gimbel DA, Nygaard HB, Gilbert JW, Strittmatter SM. Cellular prion protein mediates impairment of synaptic plasticity by amyloid-beta oligomers. Nature. 2009; 457:1128–1132. [PubMed: 19242475]
6. Zou WQ, et al. Amyloid-{beta}42 Interacts Mainly with Insoluble Prion Protein in the Alzheimer Brain. J Biol Chem. 2011; 286:15095–15105. [PubMed: 21393248]
7. Balducci C, et al. Synthetic amyloid-beta oligomers impair long-term memory independently of cellular prion protein. Proc Natl Acad Sci U S A. 2010; 107:2295–2300. [PubMed: 20133875]
8. Chen S, Yadav SP, Surewicz WK. Interaction between human prion protein and amyloid-beta (Abeta) oligomers: role OF N-terminal residues. J Biol Chem. 2010; 285:26377–26383. [PubMed: 20576610]
9. Calella AM, et al. Prion protein and Abeta-related synaptic toxicity impairment. EMBO Mol Med. 2010; 2:306–314. [PubMed: 20665634]
10. Freir DB, et al. Interaction between prion protein and toxic amyloid beta assemblies can be therapeutically targeted at multiple sites. Nat Commun. 2011; 2:336. [PubMed: 21654636]

11. Cisse M, et al. Ablation of cellular prion protein does not ameliorate abnormal neural network activity or cognitive dysfunction in the J20 line of human amyloid precursor protein transgenic mice. J Neurosci. 2011; 31:10427–10431. [PubMed: 21775587]
12. Kessels HW, Nguyen LN, Nabavi S, Malinow R. The prion protein as a receptor for amyloid-beta. Nature. 2010; 466:E3–E4. discussion E4–5. [PubMed: 20703260]
13. Gimbel DA, et al. Memory impairment in transgenic Alzheimer mice requires cellular prion protein. J Neurosci. 2010; 30:6367–6374. [PubMed: 20445063]
14. Chung E, et al. Anti-PrPC monoclonal antibody infusion as a novel treatment for cognitive deficits in an Alzheimer's disease model mouse. BMC Neurosci. 2010; 11:130. [PubMed: 20946660]
15. Resenberger UK, et al. The cellular prion protein mediates neurotoxic signalling of beta-sheet-rich conformers independent of prion replication. Embo J. 2011; 30:2057–2070. [PubMed: 21441896]
16. Barry AE, et al. Alzheimer's disease brain-derived amyloid-beta-mediated inhibition of LTP in vivo is prevented by immunotargeting cellular prion protein. J Neurosci. 2011; 31:7259–7263. [PubMed: 21593310]
17. Bate C, Williams A. Amyloid-beta-induced synapse damage is mediated via cross-linkage of cellular prion proteins. J Biol Chem. 2011; 286:37955–37963. [PubMed: 21900234]
18. You H, et al. Abeta neurotoxicity depends on interactions between copper ions, prion protein, and N-methyl-D-aspartate receptors. Proc Natl Acad Sci U S A. 2012; 109:1737–1742. [PubMed: 22307640]
19. Alier K, Ma L, Yang J, Westaway D, Jhamandas JH. Abeta inhibition of ionic conductance in mouse basal forebrain neurons is dependent upon the cellular prion protein PrPC. J Neurosci. 2011; 31:16292–16297. [PubMed: 22072680]
20. Kudo W, et al. Cellular prion protein is essential for oligomeric amyloid-beta-induced neuronal cell death. Hum Mol Genet. 2012; 21:1138–1144. [PubMed: 22100763]
21. Shankar GM, et al. Natural oligomers of the Alzheimer amyloid-beta protein induce reversible synapse loss by modulating an NMDA-type glutamate receptor-dependent signaling pathway. J Neurosci. 2007; 27:2866–2875. [PubMed: 17360908]
22. Lacor PN, et al. Abeta oligomer-induced aberrations in synapse composition, shape, and density provide a molecular basis for loss of connectivity in Alzheimer's disease. J Neurosci. 2007; 27:796–807. [PubMed: 17251419]
23. Snyder EM, et al. Regulation of NMDA receptor trafficking by amyloid-beta. Nat Neurosci. 2005; 8:1051–1058. [PubMed: 16025111]
24. Pantera B, et al. PrPc activation induces neurite outgrowth and differentiation in PC12 cells: role for caveolin-1 in the signal transduction pathway. Journal of neurochemistry. 2009; 110:194–207. [PubMed: 19457127]
25. Mouillet-Richard S, et al. Cellular prion protein signaling in serotonergic neuronal cells. Ann N Y Acad Sci. 2007; 1096:106–119. [PubMed: 17405922]
26. Williamson R, Usardi A, Hanger DP, Anderton BH. Membrane-bound beta-amyloid oligomers are recruited into lipid rafts by a fyn-dependent mechanism. FASEB J. 2008; 22:1552–1559. [PubMed: 18096814]
27. Malaga-Trillo E, et al. Regulation of embryonic cell adhesion by the prion protein. PLoS Biol. 2009; 7:e55. [PubMed: 19278297]
28. Bizat N, et al. Neuron dysfunction is induced by prion protein with an insertional mutation via a Fyn kinase and reversed by sirtuin activation in Caenorhabditis elegans. J Neurosci. 2010; 30:5394–5403. [PubMed: 20392961]
29. Suzuki T, Okumura-Noji K. NMDA receptor subunits epsilon 1 (NR2A) and epsilon 2 (NR2B) are substrates for Fyn in the postsynaptic density fraction isolated from the rat brain. Biochem Biophys Res Commun. 1995; 216:582–588. [PubMed: 7488151]
30. Grant SG, et al. Impaired long-term potentiation, spatial learning, and hippocampal development in fyn mutant mice. Science. 1992; 258:1903–1910. [PubMed: 1361685]
31. Nakazawa T, et al. Characterization of Fyn-mediated tyrosine phosphorylation sites on GluR epsilon 2 (NR2B) subunit of the N-methyl-D-aspartate receptor. J Biol Chem. 2001; 276:693–699. [PubMed: 11024032]

32. Chin J, et al. Fyn kinase induces synaptic and cognitive impairments in a transgenic mouse model of Alzheimer's disease. J Neurosci. 2005; 25:9694–9703. [PubMed: 16237174]
33. Renner M, et al. Deleterious effects of amyloid beta oligomers acting as an extracellular scaffold for mGluR5. Neuron. 2010; 66:739–754. [PubMed: 20547131]
34. Collins MO, et al. Molecular characterization and comparison of the components and multiprotein complexes in the postsynaptic proteome. Journal of neurochemistry. 2006; 97(Suppl 1):16–23. [PubMed: 16635246]
35. Stuermer CA, et al. PrPc capping in T cells promotes its association with the lipid raft proteins reggie-1 and reggie-2 and leads to signal transduction. FASEB J. 2004; 18:1731–1733. [PubMed: 15345693]
36. Salter MW, Kalia LV. Src kinases: a hub for NMDA receptor regulation. Nat Rev Neurosci. 2004; 5:317–328. [PubMed: 15034556]
37. Zhang Y, et al. Genetic reduction of striatal-enriched tyrosine phosphatase (STEP) reverses cognitive and cellular deficits in an Alzheimer's disease mouse model. Proc Natl Acad Sci U S A. 2010; 107:19014–19019. [PubMed: 20956308]
38. Prybylowski K, et al. The synaptic localization of NR2B-containing NMDA receptors is controlled by interactions with PDZ proteins and AP-2. Neuron. 2005; 47:845–857. [PubMed: 16157279]
39. Chen P, Gu Z, Liu W, Yan Z. Glycogen synthase kinase 3 regulates N-methyl-D-aspartate receptor channel trafficking and function in cortical neurons. Mol Pharmacol. 2007; 72:40–51. [PubMed: 17400762]
40. Scheff SW, DeKosky ST, Price DA. Quantitative assessment of cortical synaptic density in Alzheimer's disease. Neurobiol Aging. 1990; 11:29–37. [PubMed: 2325814]
41. Palop JJ, et al. Aberrant excitatory neuronal activity and compensatory remodeling of inhibitory hippocampal circuits in mouse models of Alzheimer's disease. Neuron. 2007; 55:697–711. [PubMed: 17785178]
42. Minkeviciene R, et al. Amyloid beta-induced neuronal hyperexcitability triggers progressive epilepsy. J Neurosci. 2009; 29:3453–3462. [PubMed: 19295151]
43. Mc Donald JM, et al. The presence of sodium dodecyl sulphate-stable Abeta dimers is strongly associated with Alzheimer-type dementia. Brain. 2010; 133:1328–1341. [PubMed: 20403962]
44. Steinerman JR, et al. Distinct pools of beta-amyloid in Alzheimer disease-affected brain: a clinicopathologic study. Arch Neurol. 2008; 65:906–912. [PubMed: 18625856]
45. Kuo YM, et al. Water-soluble Abeta (N-40, N-42) oligomers in normal and Alzheimer disease brains. J Biol Chem. 1996; 271:4077–4081. [PubMed: 8626743]
46. Peng J, et al. Semiquantitative proteomic analysis of rat forebrain postsynaptic density fractions by mass spectrometry. J Biol Chem. 2004; 279:21003–21011. [PubMed: 15020595]
47. Yoshimura Y, et al. Molecular constituents of the postsynaptic density fraction revealed by proteomic analysis using multidimensional liquid chromatography-tandem mass spectrometry. Journal of neurochemistry. 2004; 88:759–768. [PubMed: 14720225]
48. Li S, et al. Soluble A{beta} Oligomers Inhibit Long-Term Potentiation through a Mechanism Involving Excessive Activation of Extrasynaptic NR2B-Containing NMDA Receptors. J Neurosci. 2011; 31:6627–6638. [PubMed: 21543591]
49. Kojima N, Ishibashi H, Obata K, Kandel ER. Higher seizure susceptibility and enhanced tyrosine phosphorylation of N-methyl-D-aspartate receptor subunit 2B in fyn transgenic mice. Learn Mem. 1998; 5:429–445. [PubMed: 10489260]
50. Ittner LM, et al. Dendritic function of tau mediates amyloid-beta toxicity in Alzheimer's disease mouse models. Cell. 2010; 142:387–397. [PubMed: 20655099]
51. Stein PL, Lee HM, Rich S, Soriano P. pp59fyn mutant mice display differential signaling in thymocytes and peripheral T cells. Cell. 1992; 70:741–750. [PubMed: 1387588]
52. Zahn R, von Schroetter C, Wuthrich K. Human prion proteins expressed in Escherichia coli and purified by high-affinity column refolding. FEBS letters. 1997; 417:400–404. [PubMed: 9409760]

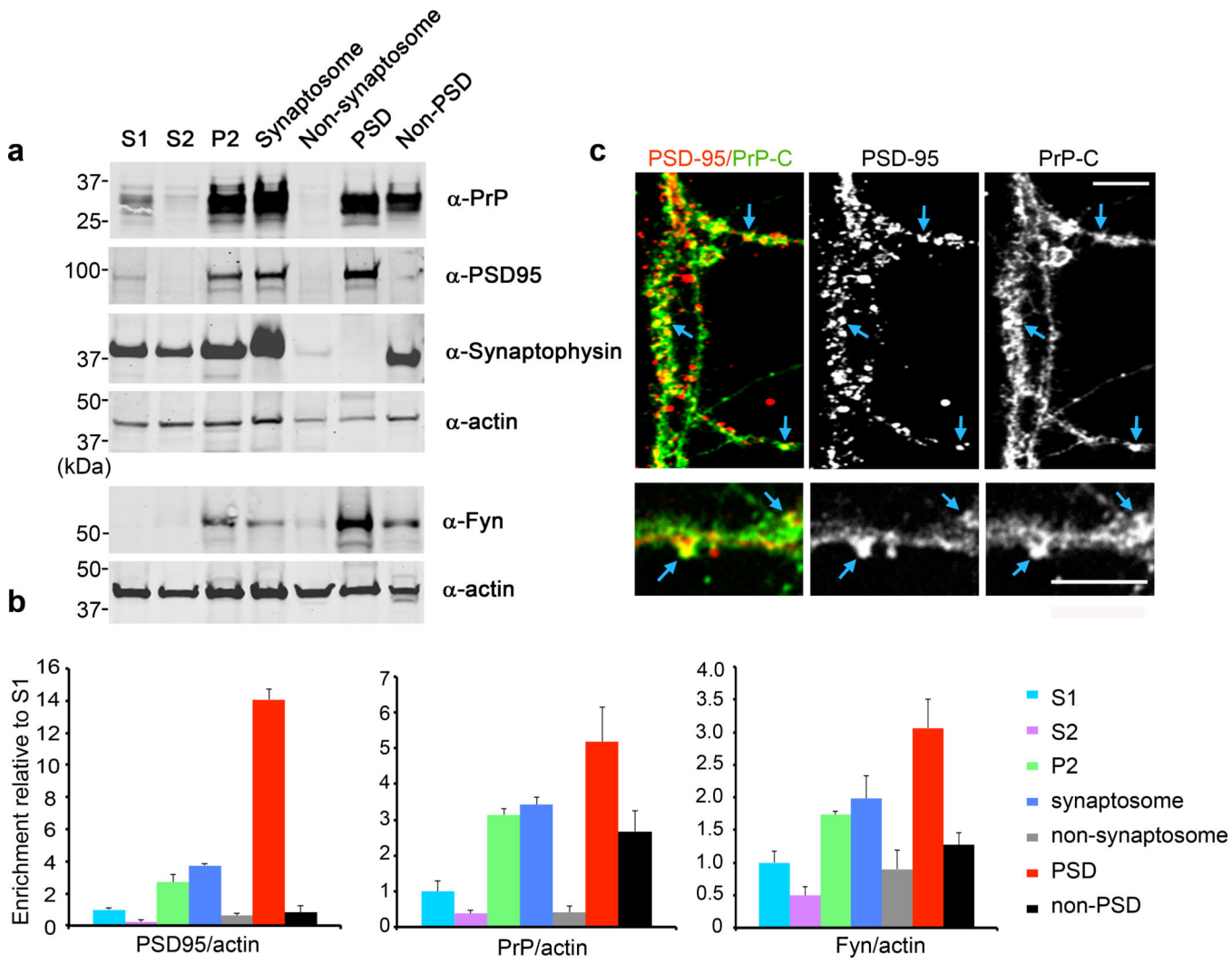

Figure 1. Localization of Prion Protein to the Post-Synaptic Density

a The indicated subcellular fractions (20 μg protein) were analyzed by immunoblot with anti-PrP^C, anti-Fyn, anti-PSD95, anti-synaptophysin, and anti-actin antibodies. The lower two panels are from a separate preparation.

b Quantification of PSD-95, PrP^C or Fyn levels normalized to actin. Data are mean ± s.e.m. for 3 independent fractionations from separate animals.

c Immunohistology of 21DIV hippocampal neurons stained with anti-PSD-95 (red in merge) and anti-PrP^C (6D11, green in merge) antibodies. Colocalization indicated by arrows. Scale bars, 4 μm.

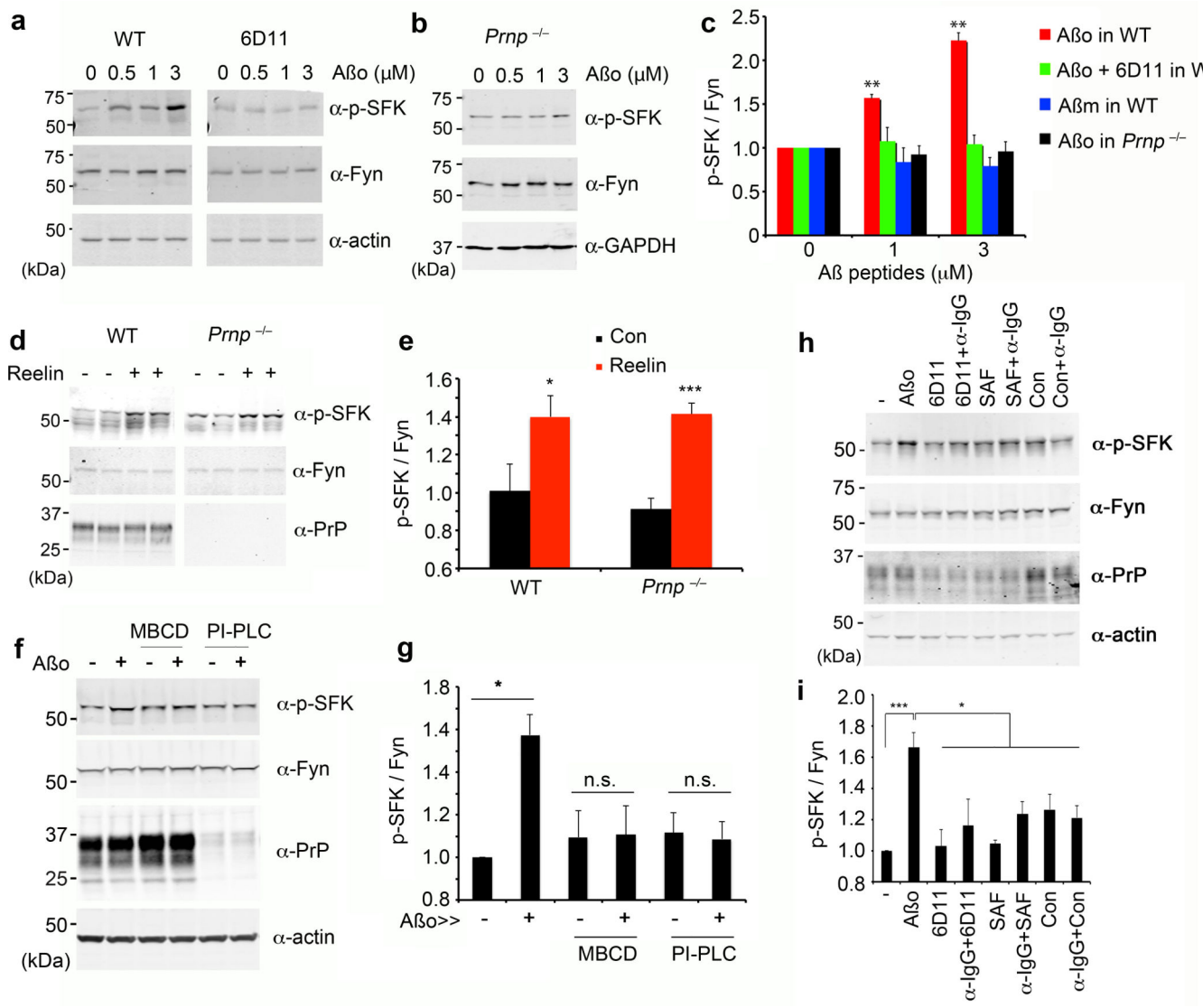

Figure 2. Aβ Oligomers Activate Fyn Kinase

a Mouse E17 WT cortical neurons at 21 DIV were treated with 0–3 μM Aβo (monomer equivalent concentration, estimated Aβo 0–30 nM) for 20 min in the absence (left panel) or presence (right panel) of 6D11 pre-incubation for 1 h. Whole cell lysates were analyzed by anti-phospho-SFK (Tyr 416) or anti-Fyn immunoblot. Actin served as a loading control.

b Cortical neurons from E17 *Prnp*$^{-/-}$ mice after 21 DIV were treated with 0–3 μM Aβo for 15 min. Lysates were analyzed by anti-phospho-SFK (Tyr 416) or anti-Fyn immunoblot. GAPDH served as a loading control.

c Quantification of phospho-SFK level in the lysate, normalized to Fyn immunoreactivity. WT, n = 4; *Prnp*$^{-/-}$, n = 4. Mean ± s.e.m. **, $P < 0.001$; one-way ANOVA (F=8.83; df=11), with Tukey post-hoc pairwise comparisons. Data normalized to 0 μM; the phospho-SFK densities without normalization at 0 μM for Aβo, Aβo+6D11, Aβm (Aβ monomer) and Aβo +*Prnp*$^{-/-}$ are 0.82±0.22, 0.86±0.10, 0.99±0.21 and 0.94±0.02.

d Cortical neurons from WT or *Prnp*$^{-/-}$ mice after 21 DIV were treated with 5 nM reelin for 25 min. Lysates analyzed by anti-phospho-SFK (Tyr 416), anti-Fyn, or anti-PrP^{C} immunoblot.

e Quantification of phospho-SFK level in the lysates (from d) normalized to Fyn immunoreactivity from 3 biologically independent experiments. Mean ± s.e.m. *, $P < 0.05$; ***, $P < 0.001$; Student's two-tailed *t* test.

f Cortical neurons from WT after 21 DIV were treated with 0–1 μM Aβo. Prior to Aβo exposure, the indicated cultures were pre-treated with 5 mg/ml methyl-β-cyclodextrin (MBCD) for 1 h or 0.1 unit of PI-PLC for 10 min. Whole cell lysates were analyzed by anti-phospho-SFK (Tyr 416), anti-Fyn, or anti-PrP^{C} immunoblot. Actin served as a loading control.

g Quantification of phospho-SFK level in the lysates (from f) normalized to Fyn immunoreactivity from 3 independent experiments. Mean ± s.e.m. *, $P < 0.05$; Student's two-tailed *t* test.

h Cortical neurons from WT after 21 DIV were treated for with 1 μM Aβo, 10 μg/ml anti-PrP^{C} antibodies (6D11 or SAF32) or control IgG (Con) antibodies, followed by adding 5 μg/ml mouse anti-IgG antibodies for crosslinking (α-IgG). Whole cell lysates were analyzed by anti-phospho-SFK (Tyr 416), anti-Fyn, or anti-PrP^{C} immunoblot. Actin served as a loading control.

i Quantification of phospho-SFK level normalized to Fyn immunoreactivity from 3 independent experiments, as in h. Mean ± s.e.m. ***, $P < 0.001$; *, $P < 0.05$; one-way ANOVA ($F=5.38$; $df=7$), Tukey post-hoc comparisons.

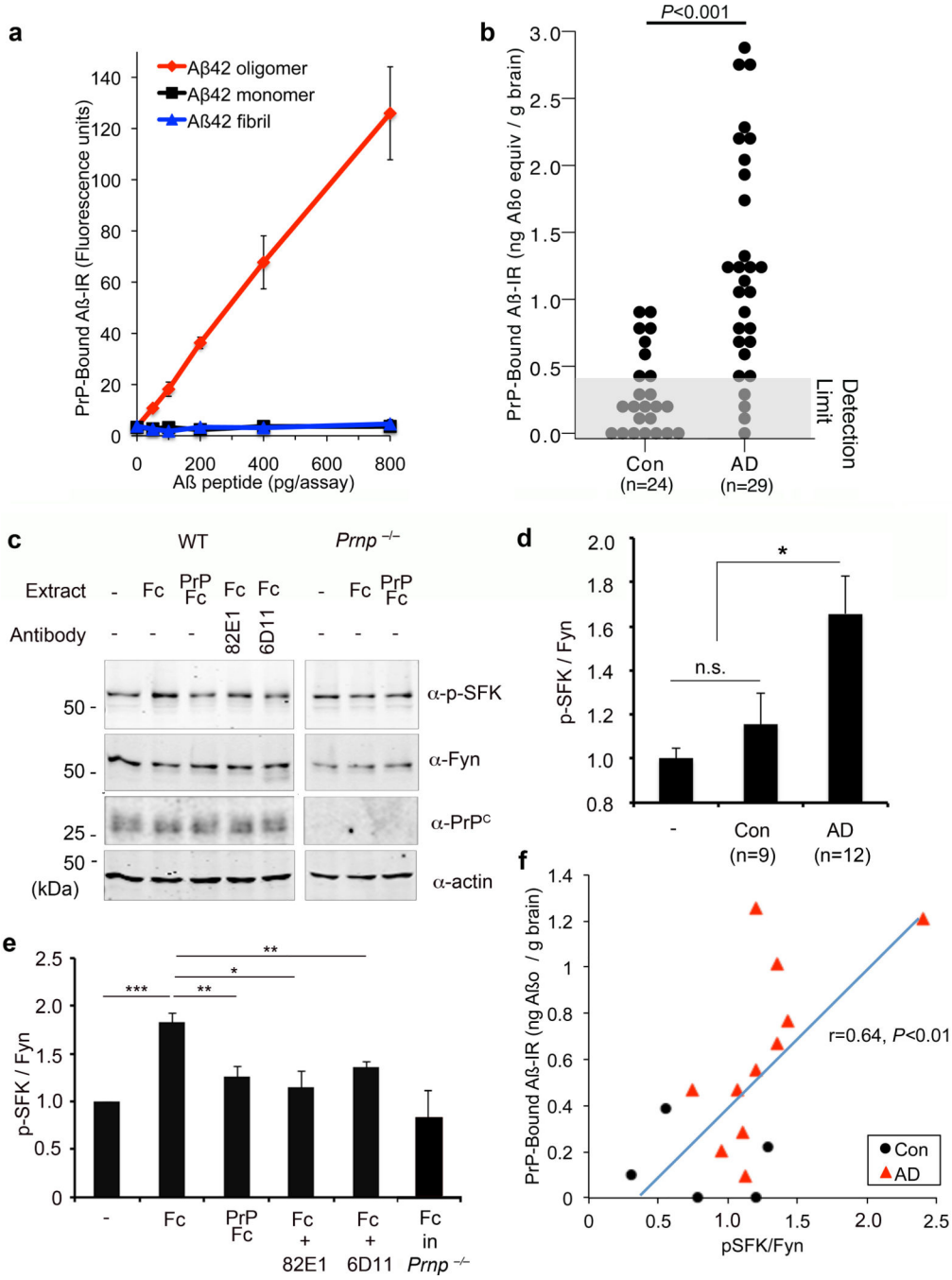

Figure 3. Aβ Species from Human AD Brain Associate with PrP^C to Activate Fyn

a Different amounts of monomer, oligomer and fibrillary Aβ were incubated with immobilized PrP(23–111). Bound Aβ was detected as time-resolved fluorescence derived from detection with anti-Aβ antibody and europium-tagged secondary reagents. Mean ± s.e.m. for 3 replicates, in one of 6 assays with similar results.

b Quantification of PrP^C-interacting Aβ species level in TBS-soluble brain extract from age-matched human control brain (Con, n=24 individuals), or human AD brain (AD, n=29).

Detection limit of the assay is shown as a gray box. $P < 0.001$; one-way ANOVA (F=20.70; df=1).

c E17 cortical neurons from WT or *Prnp*$^{-/-}$ mice after 21 DIV were treated with the indicated human AD brain extracts (6 μg total protein/ml) for 15 min. The AD brain extracts were pre-absorbed with Fc (control) or PrP-Fc resin, or incubated with 82E1 anti-Aβ antibody, or the cells were pretreated with 6D11 anti-PrP^{C} antibody, as indicated. Whole cell lysates were analyzed by anti-phospho-SFK (Tyr 416) or anti-Fyn immunoblot.

d Quantification of phospho-SFK level in the lysate, normalized to Fyn immunoreactivity. Mean ± s.e.m., human Control brain (Con), n = 9; human AD brain, n =12. *, $P < 0.05$; one-way ANOVA (F=6.58; df=2), with Tukey post-hoc comparisons.

e Quantification of phospho-SFK level in the lysate, normalized to Fyn immunoreactivity. Mean ± s.e.m., WT, n = 5; *Prnp*$^{-/-}$, n = 3 independent cultures. *, $P < 0.05$; **, $P < 0.01$; ***, $P < 0.001$; one-way ANOVA (F=8.26; df=5), with Tukey post-hoc comparisons.

f For samples analyzed for both PrP^{C}-interacting Aβ species (as in c) and Fyn activation (as in e), the correlation between the assays is plotted. Each point is from a different brain sample. Pearson coefficient of linear correlation reported with two-tailed *P*.

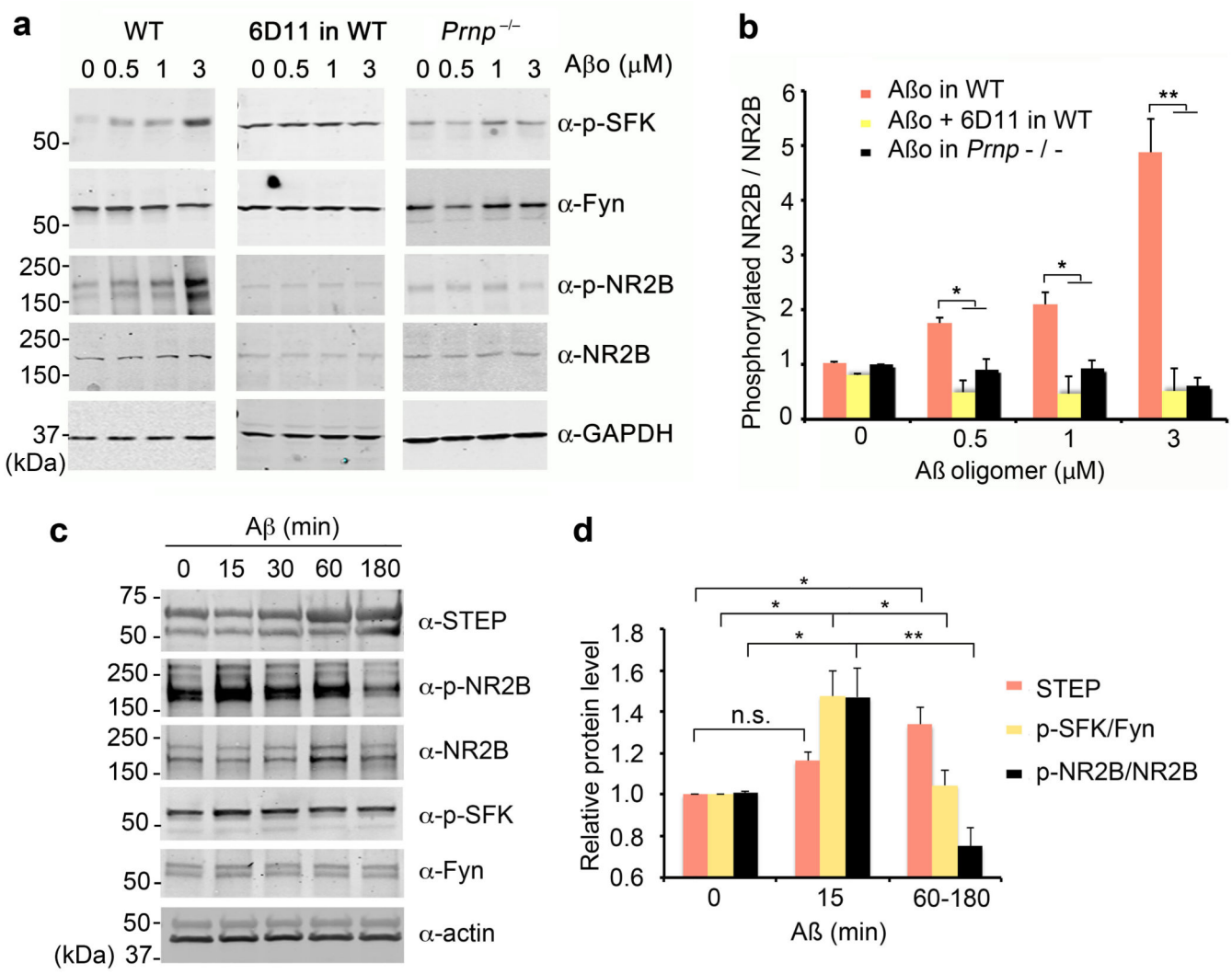

Figure 4. Aβo Increase NR2B Phosphorylation Transiently via PrP^{C} and Fyn

a Cortical neurons from E17 wild type or *Prnp*$^{-/-}$ mice after 21 DIV were treated with 0–3 μM Aβo for 20 min. Prior to Aβo exposure, the indicated cultures were pre-incubated with 10 μg/ml of 6D11 antibody for 1 h. Whole cell lysates were analyzed by anti-phospho-SFK (Tyr 416), anti-Fyn, anti-phospho-NR2B (Tyr 1472) or anti-NR2B immunoblot. GAPDH served as a loading control.

b Quantification of phospho-NR2B level in the lysate (from b) normalized to NR2B immunoreactivity. WT, n = 4; *Prnp*$^{-/-}$, n = 4. Mean ± s.e.m. *, $P < 0.05$; **, $P < 0.01$; one-way ANOVA (F=36.98; df=11), with Tukey post-hoc comparisons.

c Cortical neurons from E17 wild type after 21 DIV were treated with 1 μM Aβo for 0–180 min. Whole cell lysates were analyzed by anti-STEP, anti-phospho-NR2B (Tyr 1472), anti-NR2B, anti-phospho-SFK (Tyr 416), or anti-Fyn immunoblot. Actin served as a loading control.

d Quantification of STEP level, phospho-SFK level normalized to Fyn immunoreactivity or phospho-NR2B level in the lysate (from c) normalized to NR2B immunoreactivity. Mean ±

s.e.m. for 3 biologically independent replicates. n.s., not significant; *, $P < 0.05$; **, $P < 0.01$; one-way ANOVA (F=13.15; df=2), with Tukey post-hoc comparisons.

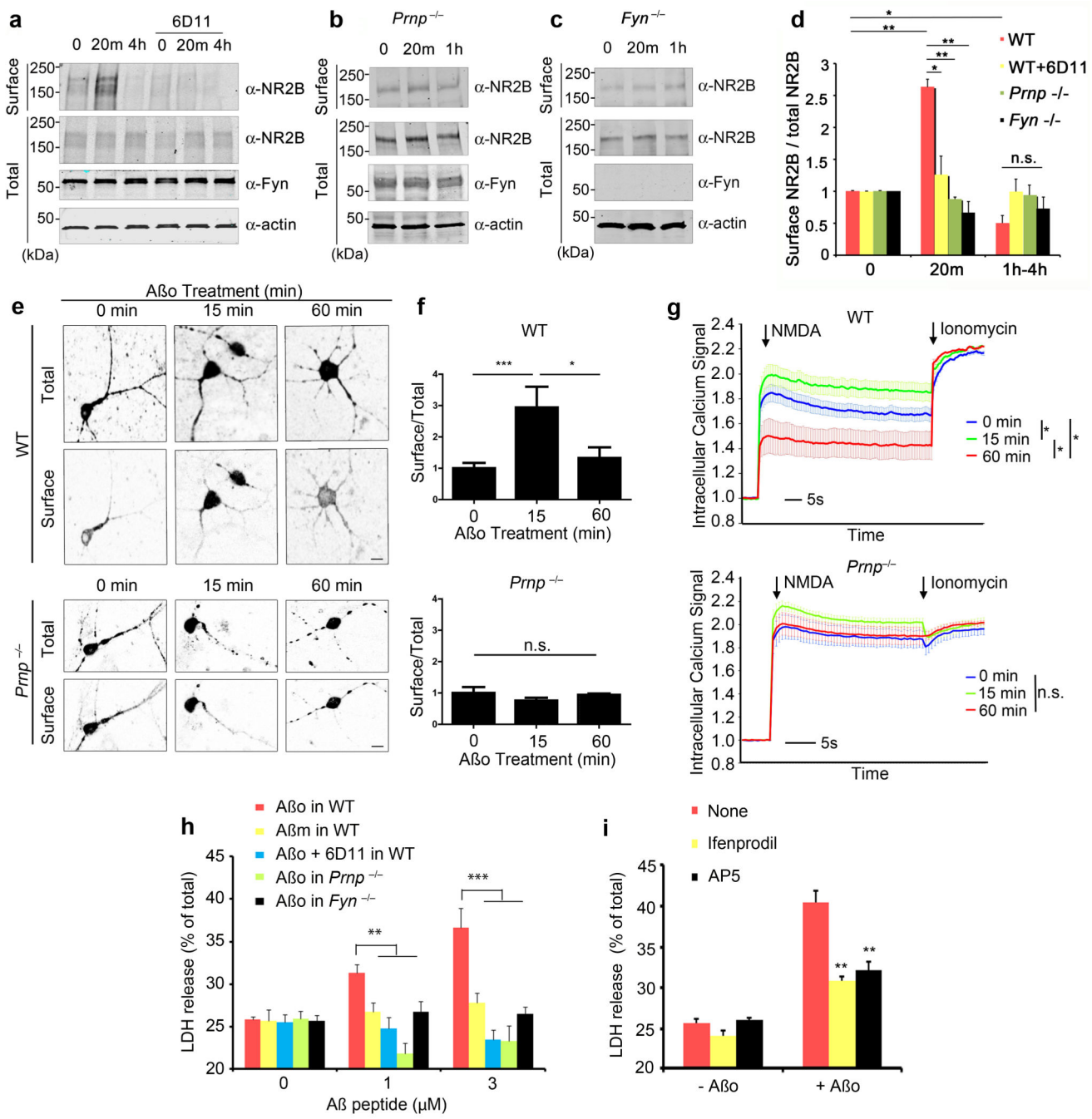

Figure 5. Aβo Induces NR2B Surface Localization, Calcium Signaling and Toxicity via PrP^C and Fyn

a–c WT, *Prnp*$^{-/-}$ or *Fyn*$^{-/-}$ E17 cortical neurons after 21 DIV were pre-incubated with or without 10 μg/ml of 6D11 antibody for 1 h, and then treated with 0–1 μM Aβo (monomer equivalent, ~10 nM oligomer) for 20 min or 4 h. Biotinylated cell surface proteins and total lysate proteins were assessed by anti-NR2B, anti-Fyn or anti-Actin immunoblot.

d Quantification of surface expression of NR2B normalized to total NR2B level. Mean ± s.e.m., WT, n = 5; *Prnp*$^{-/-}$, n = 3; *Fyn*$^{-/-}$, n = 3. *, $P < 0.05$; **, $P < 0.01$; one-way

ANOVA (F=8.02; df=11), Tukey post-hoc comparisons. Data are normalized to 0 min values; values for biotinylated NR2B in WT, WT+6D11, *Prnp*$^{-/-}$ and *Fyn*$^{-/-}$ cultures are 9.6±2.8, 9.1±2.4, 9.9±1.6 and 8.5±2.8, respectively, as a percentage of total NR2B.

e, f WT or *Prnp*$^{-/-}$ cortical neurons were transfected with expression vector encoding GFP-NR2B, and then treated with 0–1 μM Aβo for 0–60 min. Surface and total receptor were visualized. Scale bars, 10 μm. The graphs in f show the ratio of surface to total receptor as a function of time and genotype. Mean ± s.e.m., n=3 independent embryos per genotype. *, $P < 0.05$, ***, $P < 0.001$; one-way ANOVA(F=4.83; df=2), Tukey post-hoc comparisons.

g WT or *Prnp*$^{-/-}$ cortical neurons were treated with 0–1 μM Aβo for 15 or 60 min. The intracellular calcium response to NMDA (50 μM) or calcium ionophore ionomycin (500 nM) was monitored with FLIPR Calcium 4. Mean ± s.e.m., WT, n = 15 independent wells from 5 embryos; *Prnp*$^{-/-}$, n=9 independent wells from 3 embryos. *, $P < 0.05$ by Repeated Measures ANOVA (F=11.75; df=2) after NMDA addition, Tukey post-hoc comparisons. Data are normalized to pre-NMDA fluorescence; the pre-NMDA values without normalization for WT Aβo 15 m, WT Aβo 60 m, *Prnp*$^{-/-}$ Aβo 15 min and *Prnp*$^{-/-}$ Aβo 60 min are 1.05±0.11, 1.06±0.14, 1.11±0.04 and 1.13±0.12, respectively.

h WT, *Prnp*$^{-/-}$ or *Fyn*$^{-/-}$ cortical neurons at 21 DIV were treated with 0–2 μM Aβo for 1.5 h, prior to measurement of LDH release. The indicated cultures were pre-incubated with 10 μg/ml of 6D11 antibody for 1 h prior to Aβo, or were treated with Aβ monomer (Aβm) in place of Aβo. Data are mean ± s.e.m of three independent experiments. *, $P < 0.05$; **, $P < 0.01$; one-way ANOVA (F=5.73; df=14), Tukey post-hoc comparisons.

i WT neurons were pretreated with 3 μM ifenprodil or 50 μM APV for 1 h, and then Aβo was added at 1 μM. Cell toxicity after 90 min was determined by LDH release. Data represent mean ± s.e.m. from 4 independent experiments. **, $P < 0.01$; one-way ANOVA (F=70.52; df=5), Tukey post-hoc comparisons relative to no drug.

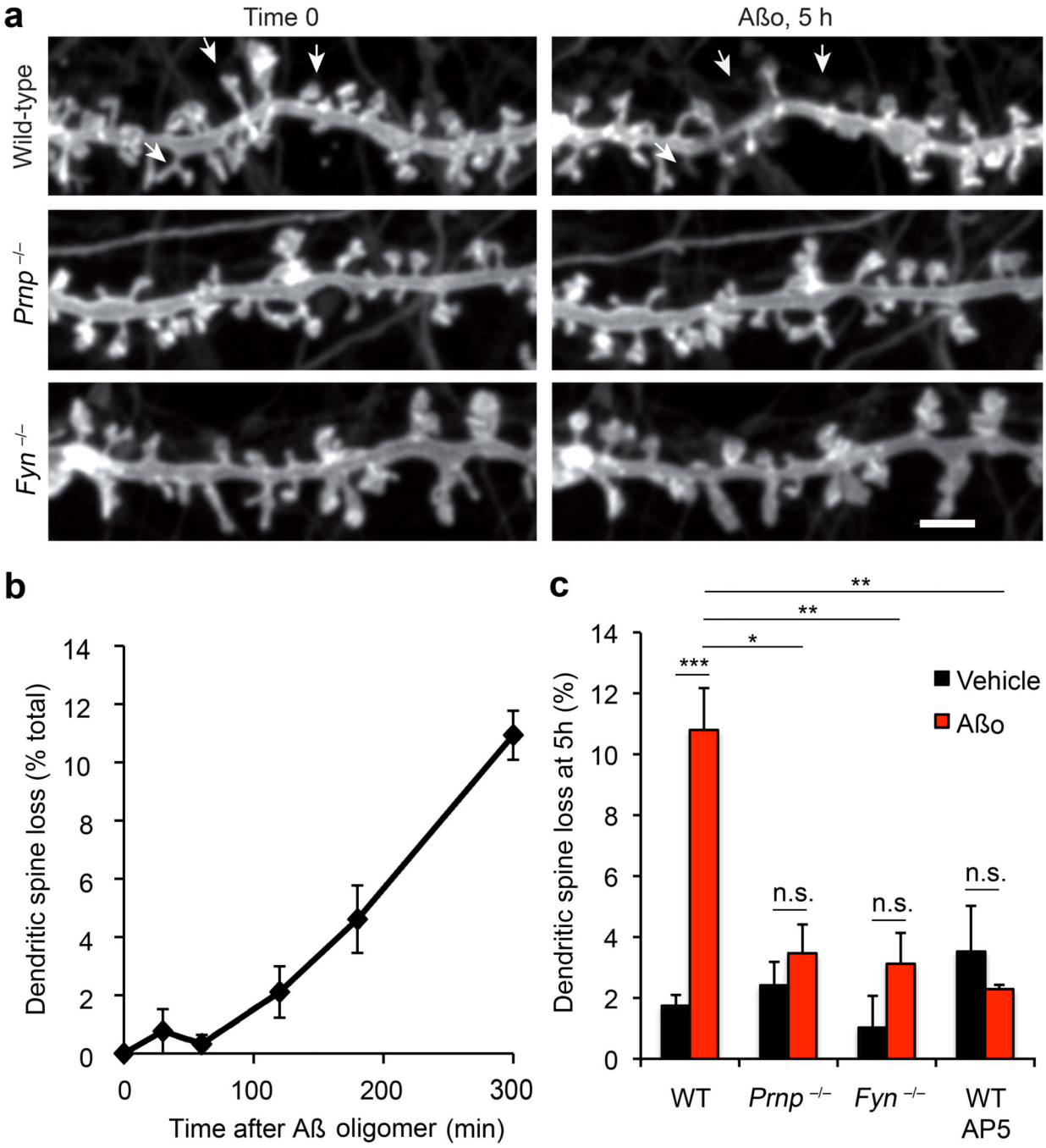

Figure 6. PrP^{C} and Fyn are Required for Aβ-Induced Dendritic Spine Loss

a Hippocampal neurons of the indicated genotypes were transfected with a Myr-EGFP expression vector and then cultured for 21 d prior to live imaging. After 1 h, 500 nM Aβo (monomer equivalent, 5 nM estimated oligomer) or vehicle was added and observations were continued for 5 h. Lost dendritic spines after Aβo addition in the WT neurons are indicated with arrowheads. Scale bar, 1 μm. A typical three-dimensional image of such spines is provided in Supplemental Movie 2.

b Dendritic spines were observed at 15 min intervals as described in a. The percentage of spines lost at the indicated times after 500 nM Aβo addition is indicated for a wild type culture. Data are mean ± sem from n = 3 separate cultures.

c Dendritic spine loss over 5 h is plotted as a function of Aβo addition and genotype. The indicated samples were incubated with 50 μM AP5 during the Aβ exposure. The data are mean ± sem from n = 12 WT, n = 3 *Prnp*$^{-/-}$, n = 3 *Fyn*$^{-/-}$, and n = 3 AP5 independent cultures from separate embryos for each genotype or drug. ***, $P < 0.001$; **, $P < 0.01$; *, $P < 0.05$; one-way ANOVA (F=8.94; df=7), Tukey post-hoc comparisons.

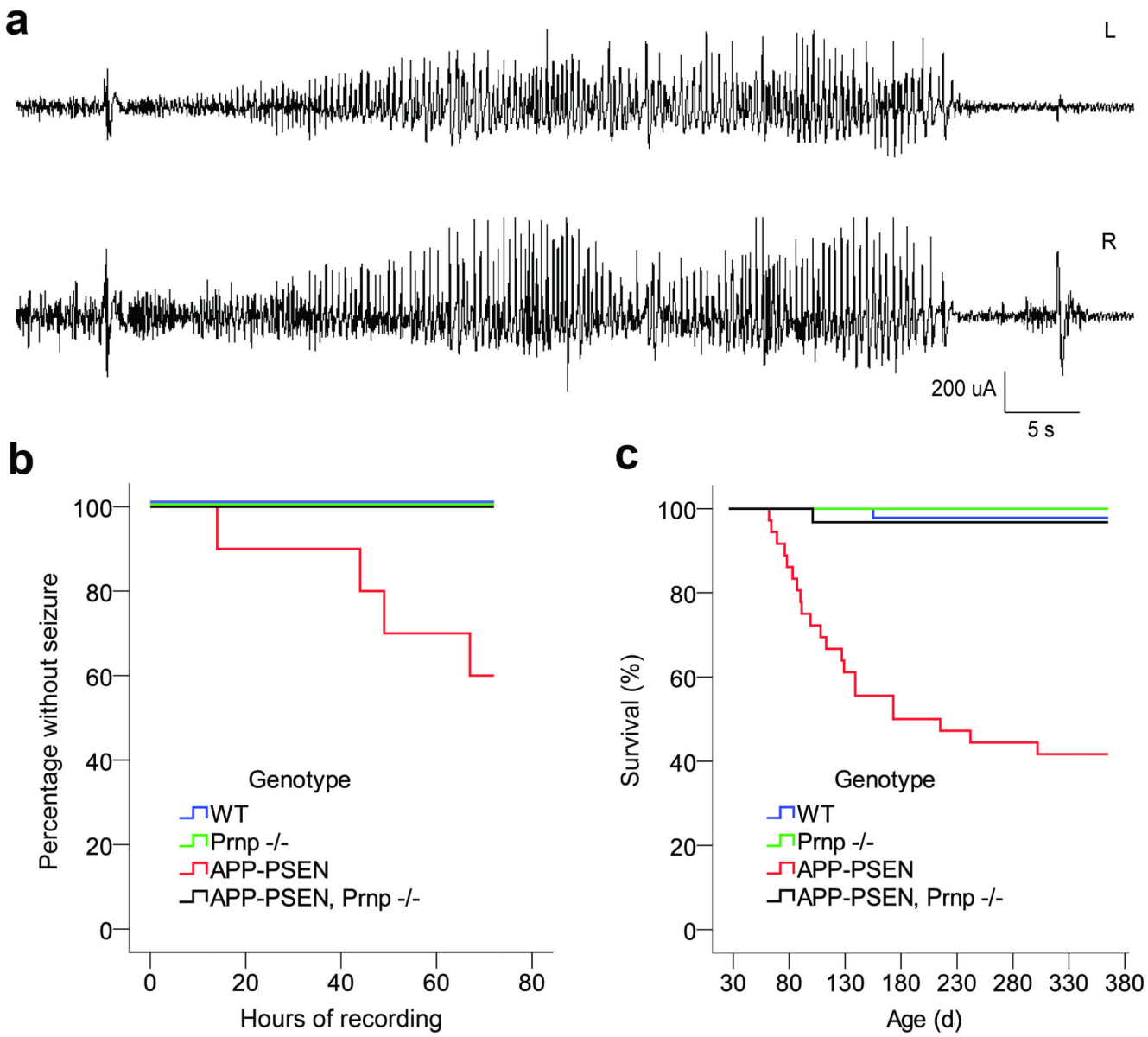

Figure 7. Seizures in Transgenic AD Mice Require PrP^{C}

a Chronic video-EEG recordings were obtained from freely moving WT, *Prnp*$^{-/-}$, APP-PSen, and APP-PSen *Prnp*$^{-/-}$ mice. Each mouse was monitored continuously for 72 h. A spontaneous seizure recorded from a transgenic Alzheimer mouse (APP-PSen). This seizure is typical in its initiation by a spike-wave discharge, and by the postictal attenuation of cerebral rhythms. L, left and R, right hemisphere signal.

b Kaplan-Meyer curve showing the latency to first seizure during 72 h of continuous EEG. Forty percent of the APP-PSen mice with normal PrP^{C} expression had at least 1 spontaneous generalized seizure during the recording session. The lack of PrP^{C} completely rescues this phenotype in transgenic APP-PSen mice (P = 0.017, Log Rank test). No seizures were recorded in WT and *Prnp*$^{-/-}$ mice. For WT n=11, *Prnp*$^{-/-}$ n=11, APP-PSen n=10, APP-Psen *Prnp*$^{-/-}$ n=12.

c Kaplan-Meyer survival curve of the mouse cohort undergoing EEG. More than 50% of transgenic mice die by 12 months age, and this phenotype is fully reversed by the lack of PrP^C expression ($P < 0.001$, Log Rank test). For WT n=46, *Prnp*$^{-/-}$ n=23, APP-PSen n=36, APP-Psen *Prnp*$^{-/-}$ n=31.